Dietary calcium (Ca^{2+}) impacts Ca^{2+} content and molecular expression of Ca^{2+}-transporters in Malpighian tubules of the yellow fever mosquito, *Aedes aegypti*

Yuan Li[1] and Peter M. Piermarini[1*]

[1]Department of Entomology, Ohio Agricultural Research and Development Center, The Ohio State University, Wooster, Ohio, United States of America

*piermarini.1@osu.edu, Wooster Science Building 250, Department of Entomology, 1680 Madison Avenue, Wooster, OH 44691; Phone: 330-263-3641.

Key words: calcium homeostasis; calcium ATPase, sodium-calcium exchanger, ion transport

Running title: Effects of dietary Ca^{2+} on mosquito renal tubules

Summary Statement: This study reveals putative roles of Malpighian tubules in regulating Ca^{2+} homeostasis of adult female mosquitoes in response to dietary Ca^{2+} loads and blood feeding.

Abstract: The renal (Malpighian) tubules of insects play important roles in hemolymph Ca^{2+} regulation. Here we provide the first investigation into how dietary Ca^{2+} loads from sucrose or blood meals affect the Ca^{2+} content and mRNA expression of Ca^{2+} transporters in Malpighian tubules of adult female mosquitoes. Using the yellow fever mosquito *Aedes aegypti* we found that feeding females for 6 days *ad libitum* on 10% sucrose with elevated Ca^{2+} concentration led to concentration-dependent increases of the Ca^{2+} content in Malpighian tubules. The increases of Ca^{2+} content correlated with up-regulations of mRNAs encoding intracellular Ca^{2+}-ATPases (*SERCA* and *SPCA*), a plasma membrane Ca^{2+}-ATPase (*PMCA*), and a K^+-dependent Na^+/Ca^{2+} exchanger (*NCKX1*). We also found that when adult females were fed blood, tubule Ca^{2+} content changed dynamically over the next 72 h in a manner consistent with redistribution of tubule Ca^{2+} stores to other tissues (e.g., ovaries). The changes in tubule Ca^{2+} were correlated with dynamic changes in mRNA abundances of *SERCA*, *SPCA*, *PMCA*, and *NCKX1*. Our results are the first to demonstrate that Malpighian tubules of adult female mosquitoes have a remarkable capacity to handle high dietary Ca^{2+} loads, most likely through the combination of storing excess Ca^{2+} within intracellular compartments and secreting it into the tubule lumen for excretion. Our results also suggest that the Malpighian tubules play key roles in supplying Ca^{2+} to other tissues during the processing of blood meals.

1. Introduction

Renal (Malpighian) tubules of insects play key roles in maintaining hemolymph osmotic and ionic balance, as well as in detoxifying and/or excreting endogenous metabolic/nitrogenous wastes and xenobiotics (Beyenbach and Piermarini, 2009; Nocelli et al., 2016). In most insects, the quintessential function of Malpighian tubules is to generate a primary urine via transepithelial fluid secretion, which is mediated by ion and water transport mechanisms in the epithelial cells (principal and stellate cells) of the distal or main segments. The primary urine flows into the proximal or lower segments, which modify the urine (e.g., by ion and/or water reabsorption) before it is emptied into the gut near the junction of the midgut and hindgut. The urine then flows through the ileum and rectum where it can be further modified before it is excreted.

In the context of ion balance, Malpighian tubules are considered the primary tissues for regulating hemolymph calcium (Ca^{2+}) concentrations. The tubule epithelium absorbs Ca^{2+} from the hemolymph and either: 1) stores it as mineralized concretions within the cells and/or tubule lumen; or 2) secretes it in soluble form into the lumen for eventual urinary excretion. In *Rhodnius prolixus* (5th stage) and *Acheta domesticus* (adult), nearly all Ca^{2+} that enters the tubules is stored within intracellular concretions; i.e., transepithelial secretion of Ca^{2+} is nominal (Maddrell et al., 1991; Browne and O'Donnell, 2018a). In adult *Drosophila melanogaster*, approximately 85% of the Ca^{2+} that enters the Malpighian tubules is stored as concretions and 15% is secreted, whereas in tubules of larval *D. melanogaster* Ca^{2+} handling is further skewed toward storage (Dube et al., 2000b; Browne and O'Donnell, 2016). The propensity of the tubules to store the majority of absorbed Ca^{2+} is likely widespread among insects given that mineralized Ca^{2+}-rich concretions have been observed in lumens and/or epithelial cells of Malpighian tubules from diverse species (Waterhouse, 1950; Clark, 1958; Bradley et al., 1990; Sohal et al., 1976; Maddrell et al., 1991; Wessing et al., 1992; Wessing and Zierold, 1999; Ballan-Dufrançais, 2002; Farina et al., 2022) and a large proportion of the total insect Ca^{2+} content (e.g., 30% in adult *D. melanogaster*, 88% in larval *Drosophila hydei*) often resides in the Malpighian tubules (Wessing and Zierold, 1992; Dube et al., 2000a).

The combined activities of Ca^{2+} storage and secretion provide Malpighian tubules with a remarkable efficiency and capacity to process hemolymph Ca^{2+}, especially among Diptera (Browne and O'Donnell, 2018b). Notably, in *D. melanogaster* and *Aedes aegypti*, it is estimated that the tubules can remove the entire hemolymph Ca^{2+} content within as little as 10 min and 18

32   min, respectively (O'Donnell and Maddrell, 1995; Browne and O'Donnell, 2018b). Accordingly,

33   experiments with flies suggest that Malpighian tubules play key roles in the processing of excess

34   dietary Ca^{2+} that is absorbed into the hemolymph by the midgut. For example, after larval fruit

35   flies (*D. hydei*) were treated with elevated dietary Ca^{2+}, the number of type-I concretions, which

36   are mainly composed of mineralized Ca^{2+}, increased in the tubule lumen (Wessing and Zierold,

37   1992). Intriguingly, when adult fruit flies (*D. melanogaster*) were fed high-Ca^{2+} diets, neither their

38   tubular Ca^{2+} content nor Ca^{2+} secretion rates were affected compared to those on standard and low

39   Ca^{2+} diets (Dube et al., 2000a). Moreover, hemolymph Ca^{2+} concentrations were unaffected,

40   suggesting the resting rates of tubular Ca^{2+} secretion were sufficient for excreting the excess Ca^{2+}

41   (Dube et al., 2000a). In another example, when adult blow flies (*Calliphora vicina*) were fed diets

42   with elevated Ca^{2+}, the Malpighian tubules showed relative increases of both Ca^{2+} content and

43   uptake rates that were nearly 2-times greater than those found in the entire body (Taylor, 1985).

44   Previous studies in Diptera suggest that Ca^{2+} stored in Malpighian tubules is not fixed; i.e.,

45   it can be mobilized to other tissues depending on the physiological demands of the insect. For

46   example, in female *C. vicina*, decreases of Malpighian tubule Ca^{2+} content were correlated with

47   commensurate increases of ovarian Ca^{2+} content, suggesting tubular Ca^{2+} stores are reabsorbed

48   into the hemolymph for use by the ovaries during reproduction (Taylor, 1984). Along similar lines,

49   in the face fly *Musca autumnalis*, development from larval to pupal stages was associated with

50   progressive decreases in tubular Ca^{2+} that coincided with quantitatively similar increases in

51   cuticular Ca^{2+} content (Krueger et al., 1988). Likewise, in *D. melanogaster* larvae, tubule Ca^{2+}

52   stores are dynamically regulated and proposed to be reabsorbed into the hemolymph for

53   maintaining hemolymph Ca^{2+} levels during periods of rapid growth and pupation (Browne and

54   O'Donnell, 2016). Thus, in the context of Ca^{2+} homeostasis, insect Malpighian tubules appear to

55   perform analogous roles as vertebrate bone.

56   To date, the cellular and molecular mechanisms of Ca^{2+} transport in insect Malpighian

57   tubules have not been fully elucidated. Electrophysiological evidence from a diversity of insect

58   species indicates that tubular Ca^{2+} uptake from the hemolymph primarily occurs across basolateral

59   membranes of the majority principal cells and not the secondary/stellate cells (Browne and

60   O'Donnell, 2018b). Consistent with this notion, mineralized intracellular concretions have only

61   been observed in principal cells (e.g., Wigglesworth and Salpeter, 1962; Sohal et al., 1976; Ryerse,

62   1979; Bradley et al., 1990; Wessing and Zierold, 1999; Beyenbach and Piermarini, 2009). A

63   variety of basolateral calcium channels (e.g., transient receptor potential, L-type, cyclic-
64   nucleotide-gated) are hypothesized to be the primary mechanisms of Ca^{2+} uptake from the
65   hemolymph (Dube et al., 2000b; MacPherson et al., 2001; Yu and Beyenbach, 2002; Browne and
66   O'Donnell, 2018a). Cytosolic Ca^{2+} is hypothesized to be stored or sequestered in intracellular
67   compartments by sarco-/endoplasmic reticulum Ca^{2+}-ATPases (SERCA) and/or secretory pathway
68   Ca^{2+}-ATPases (SPCA) (Rosay et al., 1997; Dube et al., 2000b; Yu and Beyenbach, 2002; Southall
69   et al., 2006; Davies and Terhzaz, 2009; Browne and O'Donnell, 2018a). In addition, cytosolic Ca^{2+}
70   is hypothesized to be extruded into the lumen (secretion) and/or the hemolymph (reabsorption),
71   via apical and/or basolateral plasma membrane Ca^{2+}-ATPases (PMCA), respectively (Pannabecker
72   et al., 1995; Dube et al., 2000b). A Na^+/Ca^{2+} exchange mechanism (e.g., K^+-dependent Na^+/Ca^{2+}
73   exchanger, NCKX) has also been hypothesized to contribute to the extrusion of cytosolic Ca^{2+}
74   across the apical or basolateral membranes (Dube et al., 2000b; Overend et al., 2015; Esquivel et
75   al., 2016; Li et al., 2017; Browne and O'Donnell, 2018a).

76   The goals of the present study are to generate insights into: 1) the role of the Malpighian
77   tubules in the regulation of Ca^{2+} homeostasis in adult female mosquitoes; and 2) the molecular
78   mechanisms of Ca^{2+} transport in Malpighian tubules. To date, few studies have examined the
79   physiological contributions of Malpighian tubules to Ca^{2+} homeostasis in mosquitoes. Mineralized
80   concretions have been detected in principal cells of the distal segments in larval and adult female
81   mosquitoes (Bradley and Nayar, 1985; Bradley and Nayar, 1987; Bradley et al., 1990; Beyenbach
82   and Piermarini, 2009), suggesting a potential role in Ca^{2+} storage. Moreover, high rates of Ca^{2+}
83   uptake have been measured across the basolateral membranes of principal cells in the distal
84   segment of larval *Ae. aegypti* Malpighian tubules (Browne and O'Donnell, 2018b). However, no
85   previous studies have directly examined how Malpighian tubules may contribute to Ca^{2+}
86   homeostasis in adult female mosquitoes.

87   Using the yellow fever mosquito (*Ae. aegypti*), the present study examined Ca^{2+} regulation
88   in Malpighian tubules of adult females in two independent physiological contexts. First, we
89   measured the Ca^{2+} contents of the Malpighian tubules (and whole mosquitoes) in response to
90   increased Ca^{2+} concentrations of their sucrose diet; in parallel, we quantified the molecular
91   expression of representative putative Ca^{2+} storage (SERCA, SPCA) and Ca^{2+} extrusion (PMCA,
92   NCKX) transport mechanisms in Malpighian tubules. Second, we measured the Ca^{2+} content of
93   Malpighian tubules (and whole mosquitoes) in response to a blood meal; in parallel, we quantified

94   the molecular expression of SERCA, SPCA, PMCA, and NKCX. We hypothesized that

95   Malpighian tubules would accumulate dietary Ca^{2+} (from sugar or blood meals) and that mRNAs

96   encoding Ca^{2+} transporters involved with Ca^{2+} regulation by Malpighian tubules would be

97   differentially expressed in response to dietary Ca^{2+} loading and/or blood feeding.

98

99   **2. Materials and methods**

100   **2.1. Mosquito Culture and Colony Maintenance**

101   *Ae. aegypti* (Liverpool strain) were reared as previously described (Calkins et al., 2015).

102   Mosquitoes were maintained in a growth chamber set at 27°C, 80% relative humidity, and a 12

103   h:12 h light:dark cycle. Mosquito eggs were hatched by placing them in 200 ml of distilled water

104   under vacuum for 1 h. After hatching, mosquito larvae were transferred to a 4.4 L rectangular

105   container filled with approximately 2 L of distilled water (~500 larvae per container) and provided

106   one tropical fish food tablet daily (TetraMin®, Blacksburg, VA, USA). Mosquito pupae were

107   transferred to a 12x12x12" meshed cage and adult *Ae. aegypti* were fed 10% sucrose *ad libitum*

108   after emergence. All experiments were performed on adult female mosquitoes as described in the

109   following sections. When additional eggs were needed, cages of adult females were fed

110   defibrinated rabbit blood purchased from a commercial supplier (Hemostat Laboratories, Dixon,

111   CA, USA) and provided with a coffee filter soaked in distilled water as a site for oviposition.

112   **2.2. Dietary Ca^{2+} loading and Sample Collection for Ca^{2+} Content Measurements**

113   **2.2.1. Sucrose Feeding**

114   To determine the effects of dietary Ca^{2+} loading via sucrose meals on the Ca^{2+} content of

115   tissues (Malpighian tubules, midguts) or whole bodies of adult females, various concentrations of

116    $CaCl_2$ were added to 10% sucrose. In brief, pupae were divided into several 250 ml plastic cups

117   (~100 pupae/ cup), and each group was transferred into a small cage (32-ounce Ziploc Cup with a

118   screw-on mesh lid). Before eclosion of adults, the cages were provided cotton wicks soaked in

119   10% sucrose (control) or 10% sucrose containing $CaCl_2$ (1, 5, 10, 20, 40, 50, or 80 mM). After 6

120   days, the sucrose was removed from the cage to allow any recently ingested food to be processed

121   by the mosquitoes (e.g., emptied from the crop and digested/absorbed by the midgut). 24 h after

122   removing the sucrose (on day 7), cages were placed in a refrigerator (4°C) for 5 min to immobilize

123   mosquitoes.

124   For both the control and $CaCl_2$ treated groups, Malpighian tubules and midguts were

125   isolated from 25-30 mosquitoes. Each tissue type from control and $CaCl_2$ treated groups was

126   pooled into separate 1.5 ml tubes containing 500 µl of phosphate-buffered saline (PBS; 11.9 mM

127   Phosphates, 137 mM NaCl, and 2.7 mM KCl, pH = 7.4) to represent one biological replicate. The

128   tubes were centrifuged (13,300 *rcf*) at room temperature for 5 min to pellet the tissues; the PBS

129   supernatant was then discarded. In addition, 3-5 intact females were removed from the control and

130    $CaCl_2$ treated groups and pooled together in separate 1.5 ml microcentrifuge tubes to represent one

131   biological replicate of the whole body samples. Both the tissue and whole body samples were

132   stored at -20°C until the day of analysis. At least 5 biological replicates (each derived from a

133   unique hatch of mosquito eggs) were obtained for tissue and whole body samples in both the

134   control and $CaCl_2$ treated groups.

135   **2.2.2. Blood feeding**

136   One week after emergence, a cage of ~300 adult female *Ae. aegypti* was starved for 24 h

137   by removing the 10% sucrose solution. Approximately 15 min before providing blood, ~40

138   females were removed from the cage to collect samples from a non-blood fed control group (see

139   sample collection details below). The remainder of the mosquitoes were provided access to

140   defibrinated rabbit blood (Hemostat Laboratories, Dixon, CA, USA) via a membrane feeder

141   (Hemotek, Blackburn, UK) as previously described (Calkins and Piermarini, 2017). After a 1 h

142   feeding period, the membrane feeder was removed, and all mosquitoes were immobilized on ice.

143   Mosquitoes with distended abdomens containing visible blood were selected and divided into 6

144   separate 32-ounce cages containing cotton wicks soaked in 10% sucrose (~40 females/ cage). Each

145   cage was designated for collection of tissue (Malpighian tubules, ovaries) and whole body samples

146   at a specific time point after the feeding period: 2 h, 6 h, 12 h, 24 h, 48 h, and 72 h. Malpighian

147   tubules and whole body samples were collected and pooled from non-blood fed controls and each

148   time point as described in **2.2.1**. Ovaries were isolated from 20-30 mosquitoes at each time point

149   and pooled together. The pooled tissue and whole body samples were handled and stored as

150   described in **2.2.1**. Five biological replicates (each derived from a unique hatch of mosquito eggs)

151   were obtained for each sample and time point.

152   **2.3. Measurement of Ca^{2+} Content**

153   Ca^{2+} contents of tissues and whole bodies were determined by measuring the Ca^{2+}

154   concentrations of homogenates using a Ca^{2+}-selective ion meter (HORIBA LAQUAtwin, Kyoto,

155 Japan) calibrated with $CaCl_2$ standards (0.13, 0.25, 0.50, 1.25, 2.50, 5.00 mM) dissolved in a Tris-

156 HCl buffer (i.e., 1N HCl neutralized by 2.67 M Tris-Base solution). The standards produced a

157 slope of 28.85 ± 1.0 mV/decade for sample Ca^{2+} concentrations ranging from 0.50 to 5.00 mM

158 (whole bodies and Malpighian tubules; R^2 = 0.995-1) and 26.33 ± 0.49 mV/decade for

159 concentrations ranging from 0.13 to 1.25 mM (midguts, ovaries, and defibrinated rabbit blood; R^2

160 = 0.989-0.997). The tissue or whole body samples were homogenized in 1 N HCl (100 µl per 10

161 tissues or whole body) manually using plastic pestles (Thermo Fisher Scientific Inc., Waltham,

162 MA, USA). To enhance homogenization and solubilization, the samples were incubated at 70 °C

163 for 1 h.

164 After incubation, an appropriate volume of 2.67 M Tris-Base was added to each tube to

165 reach a final Tris-Base: HCl ratio of 1:2 (v:v); this step neutralizes the pH of the sample solution,

166 which according to the manufacturer (HORIBA) is required for compatibility with the ion meter.

167 The samples were then centrifuged at 13,300 *rcf* for 5 min to pellet insoluble material and 300 µl

168 of the supernatant were applied to the recording chamber of the ion meter. The resulting voltage

169 displacement was recorded. Each sample was measured twice, and the average voltage readings

170 were compared with the standard curve to calculate sample Ca^{2+} concentrations. Ca^{2+} content in

171 nmol was then calculated from the product of the concentration and sample volume.

172 To measure the Ca^{2+} content of defibrinated rabbit blood, 100 µl of whole blood was

173 homogenized using plastic pestles in 300 µl of 1N HCl and neutralized by 150 µl of 2.67 M Tris-

174 Base. The blood samples were then centrifuged at 13,300 *rcf* for 5 min to pellet insoluble material

175 and 300 µl of the supernatant was applied to the recording chamber of the ion meter. Ca^{2+}

176 concentration and content was then determined as described above.

177 **2.4. Capillary Feeder (CAFE) Assay**

178 To estimate the amount of Ca^{2+} ingested by female mosquitoes over six days after feeding

179 on Ca^{2+}-loaded sucrose diets, capillary feeder assays were conducted, similar to those described

180 by Corfas and Vosshall (2015). In brief, three newly emerged adult female *Ae. aegypti* were placed

181 in a 28.5 x 95 mm polystyrene *Drosophila* vial (VWR International, Radnor, PA, USA) covered

182 with a cotton plug. Each vial represented one biological replicate. Two 5 µl calibrated capillary

183 tubes (VWR International) filled with 10% sucrose containing $CaCl_2$ of various concentrations

184 (see **2.2.1**) were inserted through the cotton plug. Vials with filled capillaries but no mosquitoes

185 were used to record evaporative losses. Every 24 h, the capillaries were removed from vials and

186 replaced with fresh capillaries. The distance (mm) between the starting and ending levels of the

187 removed capillary tubes were measured using a digital caliper (Traceable Carbon Fiber Caliper-

188 4″, VWR International) to determine the volume consumed (after adjusting for evaporative losses).

189 The estimated amount (nmol) of Ca^{2+} ingested per mosquito over 6 days was determined from the

190 product of the total ingested volume and Ca^{2+} concentration of the 10% sucrose.

2.5. Sample Collection for Quantitative Real-Time PCR

2.5.1. Sucrose Feeding

193 Approximately 900 mosquito pupae were divided into three groups (~300 pupae/group)

194 held in 250 ml plastic cups. Each cup was placed into an 8x8x8" cage. Within 24 h of all adults

195 emerging, cotton wicks containing 10% sucrose (control) or 10% sucrose with $CaCl_2$ (5 or 50 mM)

196 were added to the cages. At 24 h (1 day), 72 h (3 days), and 168 h (7 days) after adding the wicks,

197 Malpighian tubules were isolated from ~30 females of each cage. The Malpighian tubules were

198 pooled according to the treatment into separate 1.5 ml tubes containing PBS and centrifuged

199 (13,300 *rcf*) at 4 °C for 5 min. The supernatant was removed and 200 µl of TRIzol™ Reagent

200 (Invitrogen™, Waltham, MA, USA) was added to each tube. The tubes were stored at -80 °C until

201 the day of use. A biological replicate consisted of pooled Malpighian tubules from ~30 females

202 for each dietary Ca^{2+} concentration on each day; a total of 5 biological replicates (derived from 5

203 independent hatches) were obtained.

2.5.2. Blood feeding

205 Adult female *Ae. aegypti* were provided blood meals and Malpighian tubules were isolated

206 from ~30 females as described in **2.2.2**. The Malpighian tubules were pooled, handled, and stored

207 as described in **2.5.1**. A biological replicate consisted of Malpighian tubules from ~30 females for

208 each time point; a total of 5 biological replicates (derived from 5 independent hatches) were

209 obtained.

2.6. Quantification of mRNA expression

211 Reverse-transcriptase quantitative PCR (qPCR) was used to measure mRNA expression of

212 genes encoding four Ca^{2+}-transporters of interest in Malpighian tubules: *SERCA*, *SPCA*, *PMCA*,

213 and *NCKX1*. Total RNA was extracted from isolated Malpighian tubules as previously described

214 (Chomczynski and Sacchi, 1987). In brief, pooled Malpighian tubules were thawed on ice and

215 homogenized in 200 µl TRIzol™ Reagent using sterilized pestles. After homogenization, the total

216 RNA of each sample was extracted using the phenol-chloroform method and then treated with

217   DNase using the Turbo DNA-free™ kit (Invitrogen™). RNA concentration was determined with

218   a spectrophotometer (Nanodrop 2000, Thermo Fisher Scientific Inc.). 200 ng of total RNA from

219   each sample was reverse transcribed into cDNA using random hexamer primers and GoScript™

220   Reverse Transcriptase kit (Promega Corporation, Madison, WI, USA). The synthesized cDNA was

221   stored at -20 °C.

222   Primers to amplify approximate 100 bp regions of the Ca^{2+}-transporter cDNAs were

223   designed using Primer3 software (Table S1; Untergasser et al., 2012). Primers that amplify two

224   reference genes (*actin* and *RPS17*) established by Dzaki et al. (2017) were also utilized. All primers

225   were synthesized by Integrated DNA Technologies (IDT Inc., Morrisville, NC, USA). Standard

226   curves were used to measure the efficiency of primer amplification for each gene of interest, which

227   ranged from 98% to 102%. qPCR was performed in 96-well Multiplate™ PCR plates (Bio-Rad

228   Inc., Hercules, CA, USA) on a Real-time PCR thermocycler (Bio-Rad CFX96 Touch) at The Ohio

229   State University (OSU) Molecular and Cellular Imaging Center (MCIC) on the OSU Wooster

230   campus (Wooster, OH). Each 10 µl PCR reaction consisted of 5 µl of GoTaq® qPCR Master Mix

231   (Promega Corporation), 0.5 µl of 10 µM forward primer, 0.5 µl of 10 µM reverse primers, and 2

232   µl of cDNA template. Each PCR cycle started with an initial denaturation at 95 °C for 2 min,

233   followed by 39 cycles of 95°C (20 s), 55°C (20 s), and 68°C (20 s). A melt curve was run at the

234   end of each cycle to ensure that only a single product was amplified in each well of the qPCR

235   plate. The relative mRNA expression results were calculated using the $2^{-\Delta Ct}$ method and

236   normalized to the average Ct value of the two reference genes.

237   **2.7. Statistical analyses**

238   R (version 4.1.2), RStudio (version 2022.02.3, RStudio Inc., Boston, MA, USA), or Prism

239   (version 9; GraphPad Software Inc., La Jolla, CA, USA) were used for all statistical analyses.

240   Shapiro normality tests were conducted for each dataset; any non-normal datasets were log

241   transformed before analysis. Data figures were generated with Prism.

242   **2.7.1. Measurement of Ca^{2+} content**

243   For sucrose Ca^{2+} loading trials, the mean Ca^{2+} content of Malpighian tubules or whole

244   bodies from mosquitoes fed Ca^{2+}-treated sucrose were compared to controls using a one-way

245   analysis of variance (ANOVA) with a Holm-Sidak post hoc test (multiple comparisons were only

246   made versus the control; $p < 0.05$). For blood feeding trials, the mean Ca^{2+} content of Malpighian

247   tubules or whole bodies at each time point before and after a blood meal was compared using a

248   randomized block one-way ANOVA and Fisher's least significant difference (LSD) post hoc tests

249   ($p < 0.05$).

250   **2.7.2. Quantification of mRNA expression**

251   For dietary-Ca^{2+} loading trials, the mean mRNA expression levels of each gene of interest

252   on each day were compared between control and treatment groups using randomized block one-

253   way ANOVA and Fisher's LSD post hoc tests. For blood feeding trials, the mean mRNA

254   expression levels of each gene of interest were compared between each time point before and after

255   blood feeding using a randomized block one-way ANOVA and Fisher's LSD post hoc tests ($p <$

256   0.05).

257

258   **3. Results**

259   **3.1. Sucrose Ca^{2+} loading**

260   **3.1.1. Ca^{2+} content**

261   In adult female *Ae. aegypti* fed on 10% sucrose with nominal Ca^{2+} (controls) for 6 days,

262   the Ca^{2+} content of the Malpighian tubules (i.e., in all 5 tubules) per mosquito was 31.2 ± 2.1 nmol

263   (n = 16), representing ~18% of the whole body Ca^{2+} (172.7 ± 8.5 nmol/mosquito; n = 15). As

264   shown in Figure 1A, when mosquitoes were fed 10% sucrose containing elevated concentrations

265   of $CaCl_2$ (referred to as Ca^{2+} treatments hereafter) for 6 days, the Ca^{2+} contents of the Malpighian

266   tubules were elevated ($P < 0.05$) compared to the controls in all treatments except for 1 mM Ca^{2+}.

267   The increase of Ca^{2+} content appeared to be concentration-dependent and plateau by the 10 mM

268   Ca^{2+} treatment (Figure 1A). Similarly, whole body Ca^{2+} contents were greater ($P < 0.05$) in the

269   Ca^{2+} treatments compared to the controls, except for the 1 mM Ca^{2+} treatment (Figure 1B). The

270   increase of whole body Ca^{2+} appeared to be less concentration-dependent than that in the

271   Malpighian tubules and plateau by the 5 mM Ca^{2+} treatment (Figure 1B). The percentage of whole

272   body Ca^{2+} attributed to the Malpighian tubules increased ($P < 0.05$) in the Ca^{2+} treated groups

273   (except for 1 mM Ca^{2+}) relative to controls, reaching as much as ~38% (Figure S1). Among the

274   Ca^{2+} treatments causing significant effects (i.e., 5-80 mM), the Malpighian tubules were

275   responsible for ~37-70% of the whole body increase in Ca^{2+} (Table S2).

276   To provide a point of comparison for the Malpighian tubules, we also attempted to measure

277   the Ca^{2+} contents of midguts isolated from mosquitoes in the control and Ca^{2+} treatment groups.

278   In both mosquitoes from the control and majority of Ca^{2+} treatments, midgut Ca^{2+} contents were

279   below detectable limits of the Ca^{2+} ion meter (i.e., < 1.49 nmol per midgut). However, Ca^{2+}

280   contents of midguts from mosquitoes in the 40 and 80 mM Ca^{2+} treated mosquitoes were

281   measurable, which were 3.41 ± 0.54 (n = 5) and 6.73 ± 0.99 nmol of Ca^{2+} per midgut (n = 5)

282   respectively.

283   To provide better physiological context for the increases in whole body Ca^{2+} content

284   measured during the Ca^{2+} treatments (5-80 mM), we performed separate experiments to estimate

285   the amount of Ca^{2+} ingested in each Ca^{2+} treatment. As shown in Table S3, the estimated amount

286   of ingested Ca^{2+} exceeds the increases in the whole bodies, especially during the 10-80 mM Ca^{2+}

287   treatments. As explained in the Discussion **4.1**, we interpret the differences between these values

288   as an estimate of the amount of Ca^{2+} excreted by the mosquitoes over the experimental period

289   (Table S3).

290   **3.1.2. mRNA expression**

291   To provide insights into putative molecular mechanisms contributing to the changes in

292   Malpighian tubule Ca^{2+} content associated with dietary Ca^{2+} concentration (Figure 1A), we

293   measured mRNA expression levels of select Ca^{2+}-transporters hypothesized to contribute to

294   intracellular sequestration (SERCA, SPCA) or extrusion (PMCA, NCKX1) of cytosolic Ca^{2+}. In

295   these experiments we fed mosquitoes 10% sucrose with 5 mM or 50 mM $CaCl_2$, which correspond

296   to treatments expected to result in intermediate or maximal effects on tubule Ca^{2+} content,

297   respectively (Figure 1A); control mosquitoes were fed 10% sucrose without $CaCl_2$. The mRNA

298   expression levels of each gene in tubules of controls were stable among days 1, 3, and 7 of the

299   experiments (Figure S2). Quantiatively, *NCKX1* was the most abundant mRNA, followed by

300   *PMCA, SERCA*, and *SPCA* (Figure S2).

301   As shown in Figure 2, *SERCA* mRNA levels in Malpighian tubules of both the 5 mM and

302   50 mM Ca^{2+} treatments were up-regulated relative to those in the controls on day 3, but the change

303   was relatively small (~1.2-fold higher; Figure 2A). *SPCA* mRNAs in Malpighian tubules of the 50

304   mM Ca^{2+} treatment were elevated slighty compared to those of controls on days 1, 3, and 7 by

305   ~1.4-1.5 fold, whereas in those of 5 mM Ca^{2+} treatment, the mRNA levels of *SPCA* remained

306   unchanged relative to controls on day 1, but was up-regulated to a similar level as those of 50 mM

307   Ca^{2+} treatment on days 3 and 7 (Figure 2B). At each time point, *PMCA* mRNA levels in

308   Malpighian tubules were similar between the controls and 5 mM Ca^{2+} treatment (Figure 2C).

309   However, the mRNA abundances of *PMCA* in Malpighian tubules of the 50 mM Ca^{2+} treatment

310   were ~2-fold higher than those of the controls and the 5 mM Ca^{2+} treatments on days 1, 3, and 7

311   (Figure 2C). The mRNA levels of *NCKX1* in Malpighian tubules were similar to controls among

312   the treatments at each time point, except for day 1 when the *NCKX1* mRNA abundance was ~1.5

313   fold up-regulated in tubules of 50 mM Ca^{2+} treatment compared to those of control and 5 mM Ca^{2+}

314   treated groups (Figure 2D).

315   **3.2. Blood Feeding**

316   **3.2.1. Ca^{2+} content**

317   In non-blood fed adult female *Ae. aegypti* starved for 24 h (control), the Ca^{2+} content of

318   the Malpighian tubules per mosquito (i.e., in all 5 tubules) was 29.51± 0.81 nmol (n = 5),

319   representing ~22% of the whole body Ca^{2+} content. In blood fed *Ae. aegypti*, the Ca^{2+} contents of

320   Malpighian tubules changed dynamically over the next 72 h (Figure 3A). The Ca^{2+} content first

321   slightly increased by ~4 nmol to 33.38 ± 0.95 nmol/mosquito tubules by 6 h post-blood feeding

322   (PBF). To put this increase in context, the estimated amount of ingested Ca^{2+} from a blood meal

323   was ~3.6 nmol, assuming a typical consumption of ~3 µl of blood/female (Zhou et al., 2007) and

324   the measured Ca^{2+} concentration of defibrinated rabbit blood (~1.2 mM; see **2.2.3**).

325   Between 6-48 h PBF, the tubule Ca^{2+} content steadily decreased, reaching 17.85 ± 1.32

326   nmol/mosquito tubules by 48 h PBF (Figure 3A). This value is nearly 50% lower than tubules from

327   control mosquitoes. At 72 h PBF, the Ca^{2+} content of the tubules was similar to that at 48 h PBF

328   (Figure 3A). In contrast, the Ca^{2+} contents of whole bodies of blood-fed mosquitoes were similar

329   to those of non-blood fed controls at each time point sampled (Figure 3B). Thus, from 48-72 h

330   PBF the tubules only represented ~11% of the whole body Ca^{2+} content. The prominent decrease

331   of tubule Ca^{2+} content at 48-72 h PBF raised the question of whether it was being redistributed to

332   the ovaries as found in *C. vicina* during oogenesis (Taylor, 1984). Ca^{2+} contents of the ovaries

333   were below detectable limits (i.e., < 1.47 nmol per mosquito ovaries) in the control and majority

334   of PBF time points, but at 48 h and 72 h PBF the Ca^{2+} content of the ovaries was measurable (2.82

335   ± 0.29 nmol per mosquito ovaries; n = 5).

336   **3.2.2.   mRNA expression**

337   To provide insights into putative molecular mechanisms contributing to the dynamic

338   changes in Ca^{2+} content of Malpighian tubules after blood feeding (Figure 3), we measured the

339   transcript abundance of *SERCA, SPCA, PMCA*, and *NCKX1*. The mRNA abundance of *SERCA*

340   showed a progressive up-regulation from 2-6 h PBF reaching levels ~3-fold higher than controls

341   (Figure 4A). This elevated expression level of *SERCA* persisted until 24 h PBF and returned to

342   those of controls by 72 h PBF (Figure 4A). Similarly, *SPCA* mRNA levels were up-regulated (~1.5-

343   fold) between 6-24 h PBF and then returned progressively to control levels by 72 h PBF (Figure

344   4B). Within 2 h post-blood feeding (PBF), the mRNA abundance of *PMCA* in Malpighian tubules

345   was up-regulated (~2-fold) compared to controls and remained up-regulated through 48 h PBF

346   (Figure 4C). Between 48-72 h PBF, *PMCA* mRNA levels returned to those of controls. In contrast,

347   differential expression of *NCKX1* mRNA levels was only detected at 24 h PBF when it was ~1.5-

348   fold higher than MTs of control mosquitoes (Figure 4D).

349

350   **4. Discussion**

351   The present study is the first in adult female mosquitoes to elucidate how dietary Ca^{2+} loads

352   and blood feeding affect the Ca^{2+} content of Malpighian tubules and the molecular expression of

353   Ca^{2+} transport mechanisms in mosquito Malpighian tubules. Collectively, the results advance our

354   basic knowledge of the physiological roles that Malpighian tubules play in mosquito Ca^{2+}

355   homeostasis and putative transport mechanisms involved with the renal handling of Ca^{2+} in insects.

356   As discussed in **4.2** below, our study also reveals potential novel roles of the tubules in Ca^{2+}

357   redistribution in mosquitoes during blood meal processing and egg development.

358   **4.1. Dietary Ca^{2+} loading via sucrose**

359   When fed 10% sucrose with nominal Ca^{2+}, Malpighian tubules of adult female *Ae. aegypti*

360   contain ~18% of the whole body Ca^{2+} content. Presumably, most of the tubule and whole body

361   Ca^{2+} in adult females is derived from Ca^{2+} that was ingested during the larval stages (Barkai and

362   Williams, 1983). Supplementing the 10% sucrose with $CaCl_2$ resulted in increases of the Ca^{2+}

363   content of both Malpighian tubules and whole bodies, with the tubules responsible for the majority

364   of the whole body increases in most of the treatments. Based on previous studies in blow flies (*C.*

365   *vicina*), it is assumed that the majority of Ca^{2+} ingested by insects is absorbed into the hemolymph

366   via the midgut and then absorbed by the tubules for storage and/or excretion (Taylor, 1986). When

367   mosquitoes were fed sucrose containing ≥ 5 mM Ca^{2+}, the increases of whole body Ca^{2+} levels

368   were slightly (5 mM Ca^{2+} treatment) or dramatically (10-80 mM Ca^{2+} treatments) below the

369   estimated amounts of Ca^{2+} ingested. We hypothesize that the remaining ingested Ca^{2+} that is

370   unaccounted for in the whole bodies was excreted by the Malpighian tubules (Table S3). Taken

371   together, these findings suggest that adult female mosquitoes retain a small portion of the excess

372   dietary Ca^{2+} in the Malpighian tubules and other tissues, but once the carrying capacity of these

373   tissues is exceeded then Ca^{2+} is excreted. In other dipterans, Malpighian tubules have shown

374   similar responses to enhanced dietary Ca^{2+}; i.e., the excess is stored and/or excreted by Malpighian

375   tubules (Taylor, 1985; Wessing and Zierold, 1992; Dube et al., 2000a).

376   The above results have potential implications for adult female *Ae. aegypti* in natural

377   conditions. That is, when not blood feeding, adult female mosquitoes rely on nectar or other plant

378   juices for nutrition. A survey of nectar samples from 8 flower species determined that the Ca^{2+}

379   concentrations ranged from 0.75-13 mM (McLellan, 1975). Assuming that adult female *Ae.*

380   *aegypti* ingest flower nectar in similar quantities as 10% sucrose, our results suggest that

381   Malpighian tubules have the capacity to handle dietary Ca^{2+} loads that they would receive from

382   floral sources via storage and/or excretion.

383   Although Malpighian tubules stored large percentages of the whole body Ca^{2+} content

384   (Figure S1), especially in the elevated dietary Ca^{2+} treatments, other tissues might also contribute

385   to Ca^{2+} storage. For example, in other insects, such as adult stink bugs *Brontocoris tabidus* (Guedes

386   et al., 2007) and ants (Ballan-Dufrançais, 2002), midguts accumulate Ca^{2+}-containing granules in

387   columnar cells. Consistent with this possibility, we found that Ca^{2+} contents of midguts became

388   detectable after mosquitoes fed on high Ca^{2+} treatments (40 or 80 mM Ca^{2+}). However, compared

389   to the Malpighian tubules, the midgut Ca^{2+} levels at their highest (i.e., during the 80 mM Ca^{2+}

390   treatment) were only ~12% of that of the Malpighian tubules and represented only ~3% of the

391   whole body Ca^{2+} content.

392   The increased Ca^{2+} content of Malpighian tubules observed in the present study likely

393   corresponds to enhanced storage of mineralized Ca^{2+} within principal cells and/or tubule lumens

394   (Maddrell et al., 1991; Wessing and Zierold, 1992; Dube et al., 2000a). Consistent with potential

395   storage in principal cells, we found that Malpighian tubules of mosquitoes fed moderate (5 mM)

396   or high (50 mM) Ca^{2+} diets up-regulated both *SERCA* and *SPCA* mRNA levels. This suggests that

397   in response to elevated dietary Ca^{2+}, the tubules increase their molecular potential for transporting

398   cytosolic Ca^{2+} into intracellular storage compartments. The above interpretations are consistent

399   with previous studies in Malpighian tubules that suggest SERCA and SPCA contribute to

400   intracellular Ca^{2+} sequestration (Southall et al., 2006; Browne and O'Donnell, 2018a).

401   As previously mentioned, when fed high Ca^{2+} diets, mosquitoes likely enhance the renal

402   excretion of Ca^{2+}. Consistent with this notion, we found that Malpighian tubules of mosquitoes

403   up-regulated *PMCA* mRNAs when fed high Ca^{2+} diets. Notably, previous studies in lepidopteran

404   Malpighian tubules found PMCA-like immunoreactivity was more abundant in the apical vs.

405   basolateral membranes of principal cells (Pannabecker et al., 1995). Assuming PMCA has a

406   similar localization pattern in principal cells of mosquito Malpighian tubules, an up-regulation of

407   apical PMCA might enhance the molecular capacity of Malpighian tubules for extruding Ca^{2+}

408   across the apical membranes into the lumen for urinary excretion.

409   *NCKX1* mRNA expression in Malpighian tubules was highly abundant compared to

410   *PMCA*, *SERCA*, and *SPCA* mRNAs, consistent with findings from previous transcriptomic studies

411   (Overend et al., 2015; Esquivel et al., 2016; Li et al., 2017; Hixson et al., 2022). The localization

412   of NCKX1 protein in Malpighian tubules of any insect is unknown, but similar to PMCA, Na/Ca

413   exchange mechanisms have been hypothesized to play roles in extrusion of Ca^{2+} across both the

414   apical and basolateral membranes (Esquivel et al., 2016; Li et al., 2017; Browne and O'Donnell,

415   2018a). In this study, we found that *NCKX1* mRNA levels in mosquito Malpighian tubules were

416   transiently up-regulated on day 1 in response to the high dietary Ca^{2+} treatment before returning

417   to control levels on days 3 and 7. Thus, it is possible that NCKX1 is specialized for enhancing

418   Ca^{2+} excretion during the acute stages of the high Ca^{2+} treatment, presumably via apical secretion.

419   Figure 5 presents a hypothetical model of Ca^{2+} transport in mosquito Malpighian tubules that

420   illustrates our interpretations of the above molecular changes in response to elevated dietary Ca^{2+}

421   from sucrose meals.

422   **4.2. Blood feeding**

423   Our study is the first to provide insights into how the Ca^{2+} content of Malpighian tubules

424   in mosquitoes is affected during blood meal processing and egg development. Notably, the Ca^{2+}

425   content of Malpighian tubules was dynamic within 72 h after ingesting blood and appeared to

426   consist of 3 distinct phases. The first phase (0-6 h PBF) was characterized by a small increase of

427   Ca^{2+} that was remarkably similar to the estimated amount of Ca^{2+} in the ingested blood (i.e., ~3.6

428   nmol), suggesting the Malpighian tubules are a sink for nearly all of the ingested Ca^{2+} in the blood

429   meal. Similarly, in the obligate-hematophagous *R. prolixus*, most of the Ca^{2+} from ingested blood

430   was deposited in the upper segments of Malpighian tubules (Maddrell et al., 1991).

431   The second phase (6-48 h PBF) was characterized by a dramatic decrease in the Ca^{2+}

432   content of the tubules by ~50%, whereas the third phase (48-72 h PBF) was characterized by a

433   stasis of tubule Ca^{2+} levels. Given that the whole body Ca^{2+} content did not change during phase

434 2, the decrease in tubule Ca^{2+} content likely reflects its redistribution from mineralized stores to

435 other tissues rather than excretion from the mosquito. One potential site for redistribution of tubule

436 Ca^{2+} is the ovaries (Taylor, 1984). Consistent with this notion, ovarian Ca^{2+} levels were not

437 detectable until the end of phase 2 and remained stable through phase 3, accounting for ~20% of

438 the decreased tubule Ca^{2+} content. The tissues responsible for the remaining ~80% of the decreased

439 tubule Ca^{2+} content remain to be determined.

440 The timing of reduced tubule and increased ovarian Ca^{2+} contents overlaps with

441 vitellogenesis in *Ae. aegypti*, which typically peaks between 24-30 h PBF and ends by 48 h PBF

442 (Dhadialla et al., 1992). Ca^{2+} plays an important role in the signaling of ovaries during

443 vitellogenesis (Dhadialla and Raikhel, 1991; Sappington and S. Raikhel, 1998; Warrier and

444 Subramoniam, 2002). Thus, the changes in tubule and ovarian Ca^{2+} contents during phase 2 may

445 reflect an important role of tubule Ca^{2+} stores in maintaining hemolymph Ca^{2+} levels to

446 accommodate the demands of the ovaries and other tissues that undergo intensive Ca^{2+} cell

447 signaling during vitellogenesis. At least in vertebrate systems, cells undergoing intensive

448 intracellular Ca^{2+} signaling have been shown to decrease the Ca^{2+} concentrations of the

449 surrounding extracellular fluid (Hofer, 2005).

450 Our qPCR results revealed that the dynamic changes in Ca^{2+} content after blood feeding

451 coincided with dynamic changes in Ca^{2+}-transporter mRNA expression. That is, *SERCA* and *SPCA*

452 were up-regulated during phase 1, suggesting the tubules enhance their molecular potential to store

453 intracellular Ca^{2+} as ingested Ca^{2+} is absorbed into the hemolymph. On the other hand, SERCA

454 and SPCA were down-regulated during phases 2 and 3, suggesting the tubules decrease their

455 molecular potential to store intracelluar Ca^{2+} while tubule Ca^{2+} stores are being reduced for use by

456 other tissues (e.g., ovaries).

457 *PMCA* transcripts showed a similar pattern of up-regulation as *SERCA* and *SPCA*, but

458 remained up-regulated throughout phase 2, before returning to control levels by phase 3. On the

459 other hand, *NCKX1* transcripts showed a gradual up-regulation that did not peak until the middle

460 of phase 2 (24 h PBF), followed by a down-regulation to control levels by the end of phase 3.

461 Taken together, these findings suggest the tubules maximize their molecular potential to extrude

462 cytosolic Ca^{2+} during phase 2, consistent with the 50% decrease in tubule Ca^{2+} content. Given that

463 tubule Ca^{2+} is more likely redstributed to other tissues rather than excreted during phase 2, we

464 hypothesize that the up-regulation of *PMCA* and *NCKX1* mRNAs leads to enhanced basolateral

bioRxiv preprint doi: https://doi.org/10.1101/2023.03.30.534971; this version posted April 3, 2023. The copyright holder for this preprint (which was not certified by peer review) is the author/funder, who has granted bioRxiv a license to display the preprint in perpetuity. It is made available under aCC-BY-NC-ND 4.0 International license.

465   PMCA and NCKX1 protein abundances in Malpighian tubules, which would be expected to

466   enhance the reabsorption of cytosolic Ca^{2+} (presumably released from intracellular stores) into the

467   hemolymph during phase 2 for eventual use by other tissues (e.g., ovaries). Moreover, the down-

468   regulation of putative basolateral PMCA and NCKX1 by phase 3 would coincide with reduced

469   demand/use of tubule Ca^{2+} by other tissues (e.g., ovaries) post-vitelleogensis. Figure 6 presents a

470   hypothetical model of Ca^{2+} transport in mosquito Malpighian tubules that illustrates our

471   interpretations of the above molecular changes after blood feeding during phases 1 and 2.

472   In conclusion, the results of our study suggest that Malpighian tubules have a remarkable

473   capacity to handle excess dietary Ca^{2+} in sucrose meals, most likely by first storing Ca^{2+} (via up-

474   regulated intracellular *SERCA* and *SPCA*) and then secreting it (via up-regulated apical *PMCA* and

475   *NCKX1)* once storage capacity is reached. We also found that after ingesting blood the Ca^{2+} levels

476   in Malpighian tubules are dynamic, likely responding to metabolic demands for Ca^{2+} in other

477   tissues (e.g., ovaries) by modulating the molecular capacity of the tubules for intracellular storage

478   (*SERCA*, *SPCA*) and basolateral reabsorption (*PMCA*, *NCKX1*) of Ca^{2+}. Future studies will be

479   required to confirm the hypothesized localizations of the above Ca^{2+} transport mechanisms and

480   functional changes in Malpighian tubules in response to elevated dietary Ca^{2+} treatments or blood

481   feeding. Given the indispensable roles of Ca^{2+} in insect physiology, additional studies investigating

482   Ca2+ processing by Malpighian tubules and their underlying Ca^{2+} transport mechanisms may also

483   reveal novel biochemical targets for developing insecticides that disrupt the renal regulation of

484   Ca^{2+} homeostasis in mosquitoes.

485

487   The authors thank Dr. Ellen Klinger (OSU) and Dr. Tae Young Lee (OSU) for providing

488   guidance on statistical analyses, Dr. Ana Trabanino (OSU) for assistance with RT-qPCR

489   expreiments, and Dr. Mike O'Donnell (McMaster University) for helpful discussions and insights.

490

6. References

Ballan-Dufrançais, C. (2002). Localization of metals in cells of pterygote insects: Metals in Cells of Insects. *Microsc. Res. Tech.* **56**, 403–420.

Barkai, A. I. and Williams, R. W. (1983). The exchange of calcium in larvae of the mosquito Aedes aegypti. *Journal of Experimental Biology* **104**, 139–148.

Beyenbach, K. and Piermarini, P. (2009). Osmotic and Ionic Regulation in Insects. In *Osmotic and Ionic Regulation* (ed. Evans, D.), pp. 231–293. CRC Press.

Bradley, T. J. and Nayar, J. K. (1985). Intracellular melanization of the larvae of Dirofilaria immitis in the Malpighian tubules of the mosquito, Aedes sollicitans. *Journal of Invertebrate Pathology* **45**, 339–345.

Bradley, T. J. and Nayar, J. K. (1987). An Ultrastructural Study of Dirofilaria immitis Infection in the Malpighian Tubules of Anopheles quadrimaculatus. *The Journal of Parasitology* **73**, 1035–1043.

Bradley, T. J., Nayar, J. K. and Knight, J. W. (1990). Selection of a strain of Aedes aegypti susceptible to Dirofilaria immitis and lacking intracellular concretions in the Malpighian tubules. *Journal of Insect Physiology* **36**, 709–717.

Browne, A. and O'Donnell, M. J. (2016). Segment-specific Ca 2+ transport by isolated Malpighian tubules of Drosophila melanogaster : A comparison of larval and adult stages. *Journal of Insect Physiology* **87**, 1–11.

Browne, A. and O'Donnell, M. J. (2018a). Mechanisms of calcium sequestration by isolated Malpighian tubules of the house cricket Acheta domesticus. *Arch. Insect Biochem. Physiol.* **97**, e21431.

Browne, A. and O'Donnell, M. J. (2018b). Calcium transport across the basolateral membrane of isolated Malpighian tubules: a survey of several insect orders: Calcium transport by Malpighian tubules. *Physiol. Entomol* **43**, 227–238.

516   **Calkins, T. L. and Piermarini, P. M.** (2017). A Blood Meal Enhances Innexin mRNA
517   Expression in the Midgut, Malpighian Tubules, and Ovaries of the Yellow Fever
518   Mosquito Aedes aegypti. *Insects* **8**, 122.

519   **Calkins, T. L., Woods-Acevedo, M. A., Hildebrandt, O. and Piermarini, P. M.** (2015). The
520   molecular and immunochemical expression of innexins in the yellow fever mosquito,
521   Aedes aegypti: Insights into putative life stage- and tissue-specific functions of gap
522   junctions. *Comparative Biochemistry and Physiology Part B: Biochemistry and*
523   *Molecular Biology* **183**, 11–21.

524   **Chomczynski, P. and Sacchi, N.** (1987). Single-step method of RNA isolation by acid
525   guanidinium thiocyanate-phenol-chloroform extraction. *Analytical Biochemistry* **162**,
526   156–159.

527   **Clark, E. W.** (1958). A Review of Literature on Calcium and Magnesium in Insects. *Annals of*
528   *the Entomological Society of America* **51**, 142–154.

529   **Corfas, R. A. and Vosshall, L. B.** (2015). The cation channel TRPA1 tunes mosquito
530   thermotaxis to host temperatures. *eLife* **4**, e11750.

531   **Davies, S. A. and Terhzaz, S.** (2009). Organellar calcium signalling mechanisms in Drosophila
532   epithelial function. *Journal of Experimental Biology* **212**, 387–400.

533   **Dhadialla, T. S. and Raikhel, A. S.** (1991). Binding of vitellogenin to membranes isolated from
534   mosquito ovaries. *Archives of Insect Biochemistry and Physiology* **18**, 55–70.

535   **Dhadialla, T. S., Hays, A. R. and Raikhel, A. S.** (1992). Characterization of the solubilized
536   mosquito vitellogenin receptor. *Insect Biochemistry and Molecular Biology* **22**, 803–816.

537   **Dube, K. A., McDonald, D. G. and O'Donnell, M. J.** (2000a). Calcium homeostasis in larval
538   and adult Drosophila melanogaster. *Arch. Insect Biochem. Physiol.* **44**, 27–39.

539   **Dube, K., McDonald, D. G. and O'Donnell, M. J.** (2000b). Calcium transport by isolated
540   anterior and posterior Malpighian tubules of Drosophila melanogaster: roles of
541   sequestration and secretion. *Journal of Insect Physiology* **46**, 1449–1460.

542 **Dzaki, N., Ramli, K. N., Azlan, A., Ishak, I. H. and Azzam, G.** (2017). Evaluation of reference
543   genes at different developmental stages for quantitative real-time PCR in Aedes aegypti.
544   *Sci Rep* **7**, 43618.

545 **Esquivel, C. J., Cassone, B. J. and Piermarini, P. M.** (2016). A de novo transcriptome of the
546   Malpighian tubules in non-blood-fed and blood-fed Asian tiger mosquitoes Aedes
547   albopictus: insights into diuresis, detoxification, and blood meal processing. *PeerJ* **4**,
548   e1784.

549 **Farina, P., Bedini, S. and Conti, B.** (2022). Multiple Functions of Malpighian Tubules in
550   Insects: A Review. *Insects* **13**, 1001.

551 **Guedes, B. A. M., Zanuncio, J. C., Ramalho, F. S. and Serrão, J. E.** (2007). Midgut
552   morphology and enzymes of the obligate zoophytophagous stinkbug Brontocoris tabidus
553   (Signoret, 1863) (Heteroptera: Pentatomidae). *Pan-Pacific Entomologist* **83**, 66–74.

554 **Hixson, B., Bing, X.-L., Yang, X., Bonfini, A., Nagy, P. and Buchon, N.** (2022). A
555   transcriptomic atlas of Aedes aegypti reveals detailed functional organization of major
556   body parts and gut regional specializations in sugar-fed and blood-fed adult females.
557   *eLife* **11**, e76132.

558 **Hofer, A. M.** (2005). Another dimension to calcium signaling: a look at extracellular calcium.
559   *Journal of Cell Science* **118**, 855–862.

560 **Krueger, R. A., Broce, A. B., Hopkins, T. L. and Kramer, K. J.** (1988). Calcium transport
561   from Malpighian tubules to puparial cuticle ofMusca autumnalis. *J Comp Physiol B* **158**,
562   413–419.

563 **Li, Y., Piermarini, P. M., Esquivel, C. J., Drumm, H. E., Schilkey, F. D. and Hansen, I. A.**
564   (2017). RNA-Seq Comparison of Larval and Adult Malpighian Tubules of the Yellow
565   Fever Mosquito Aedes aegypti Reveals Life Stage-Specific Changes in Renal Function.
566   *Frontiers in Physiology* **8**,.

567 **MacPherson, M. R., Pollock, V. P., Broderick, K. E., Kean, L., O'Connell, F. C., Dow, J. A.**
568   **T. and Davies, S. A.** (2001). L-type calcium channels regulate epithelial fluid transport

569   in Drosophila melanogaster. *American Journal of Physiology-Cell Physiology* **280**,

570   C394–C407.

571 **Maddrell, S. H. P., Whittembury, G., Mooney, R. L., Harrison, J. B., Overton, J. A. and**

572   **Rodriguez, B.** (1991). The fate of calcium in the diet of Rhodnius prolixus: storage in

573   concretion bodies in the Malpighian tubules. 20.

574 **McLellan, A. R.** (1975). Calcium, Magnesium, Potassium, and Sodium in Honey and in Nectar

575   Secretion. *Journal of Apicultural Research* **14**, 57–61.

576 **Nocelli, R. C., Cintra-Socolowski, P., Roat, T. C., Silva-Zacarin, E. C. and Malaspina, O.**

577   (2016). Comparative physiology of Malpighian tubules: form and function. *OAIP* **6**, 13–

578   23.

579 **O'Donnell, M. J. and Maddrell, S. H.** (1995). Fluid reabsorption and ion transport by the lower

580   Malpighian tubules of adult female Drosophila. *Journal of Experimental Biology* **198**,

581   1647–1653.

582 **Overend, G., Cabrero, P., Halberg, K. A., Ranford-Cartwright, L. C., Woods, D. J., Davies,**

583   **S. A. and Dow, J. A. T.** (2015). A comprehensive transcriptomic view of renal function

584   in the malaria vector, Anopheles gambiae. *Insect Biochemistry and Molecular Biology*

585   **67**, 47–58.

586 **Pannabecker, T. L., Smith, C. A., Beyenbach, K. W. and Wasserman, R. H.** (1995).

587   Immunocytochemical localization of a plasma membrane calcium pump in the insect

588   (Lymantria dispar) Malpighian tubule. *Journal of Insect Physiology* **41**, 1105–1112.

589 **Rosay, P., Davies, S. A., Yu, Y., Sozen, A., Kaiser, K. and Dow, J. A.** (1997). Cell-type

590   specific calcium signalling in a Drosophila epithelium. *Journal of Cell Science* **110**,

591   1683–1692.

592 **Ryerse, J. S.** (1979). Developmental changes in Malpighian tubule cell structure. *Tissue Cell* **11**,

593   533–551.

594 **Sappington, T. W. and S. Raikhel, A.** (1998). Molecular characteristics of insect vitellogenins
595   and vitellogenin receptors. *Insect Biochemistry and Molecular Biology* **28**, 277–300.

596 **Sohal, R. S., Peters, P. D. and Hall, T. A.** (1976). Fine structure and X-ray microanalysis of
597   mineralized concretions in the Malpighian tubules of the housefly, Musca domestica.
598   *Tissue and Cell* **8**, 447–458.

599 **Southall, T. D., Terhzaz, S., Cabrero, P., Chintapalli, V. R., Evans, J. M., Dow, J. A. T. and**
600   **Davies, S.-A.** (2006). Novel subcellular locations and functions for secretory pathway
601   Ca2+/Mn2+-ATPases. *Physiological Genomics* **26**, 35–45.

602 **Taylor, C. W.** (1984). Calcium distribution during egg development in Calliphora vicina.
603   *Journal of Insect Physiology* **30**, 905–910.

604 **Taylor, C. W.** (1985). Calcium regulation in blowflies: absence of a role for midgut. *American*
605   *Journal of Physiology-Regulatory, Integrative and Comparative Physiology* **249**, R209–
606   R213.

607 **Taylor, C. W.** (1986). Calcium Regulation in Insects. In *Advances in Insect Physiology*, pp.
608   155–186. Elsevier.

609 **Warrier, S. and Subramoniam, T.** (2002). Receptor mediated yolk protein uptake in the crab
610   Scylla serrata: crustacean vitellogenin receptor recognizes related mammalian serum
611   lipoproteins. *Molecular Reproduction and Development* **61**, 536–548.

612 **Waterhouse, D. F.** (1950). Studies of the Physiology and Toxicology of Blowflies. *Aust. Jnl. Of*
613   *Bio. Sci.* **3**, 76–112.

614 **Wessing, A. and Zierold, K.** (1992). Metal-salt feeding causes alterations in concretions in
615   Drosophila larval Malpighian tubules as revealed by X-ray microanalysis. *Journal of*
616   *Insect Physiology* **38**, 623–632.

617 **Wessing, A. and Zierold, K.** (1999). The formation of type-I concretions in Drosophila
618   Malpighian tubules studied by electron microscopy and X-ray microanalysis. *Journal of*
619   *Insect Physiology* **45**, 39–44.

620 **Wessing, A., Zierold, K. and Hevert, F.** (1992). Two types of concretions in Drosophila
621   Malpighian tubules as revealed by X-ray microanalysis: A study on urine formation.
622   *Journal of Insect Physiology* **38**, 543–554.

623 **Wigglesworth, V. B. and Salpeter, M. M.** (1962). Histology of the Malpighian tubules in
624   Rhodnius prolixus Stål (Hemiptera). *Journal of Insect Physiology* **8**, 299–307.

625 **Yu, M.-J. and Beyenbach, K. W.** (2002). Leucokinin activates Calcium -dependent signal
626   pathway in principal cells of Aedes aegypti Malpighian tubules. *American Journal of*
627   *Physiology-Renal Physiology* **283**, F499–F508.

628 **Zhou, G., Kohlhepp, P., Geiser, D., Frasquillo, M. del C., Vazquez-Moreno, L. and**
629   **Winzerling, J. J.** (2007). Fate of blood meal iron in mosquitoes. *Journal of Insect*
630   *Physiology* **53**, 1169–1178.

631   ## 7. Figures and Legends
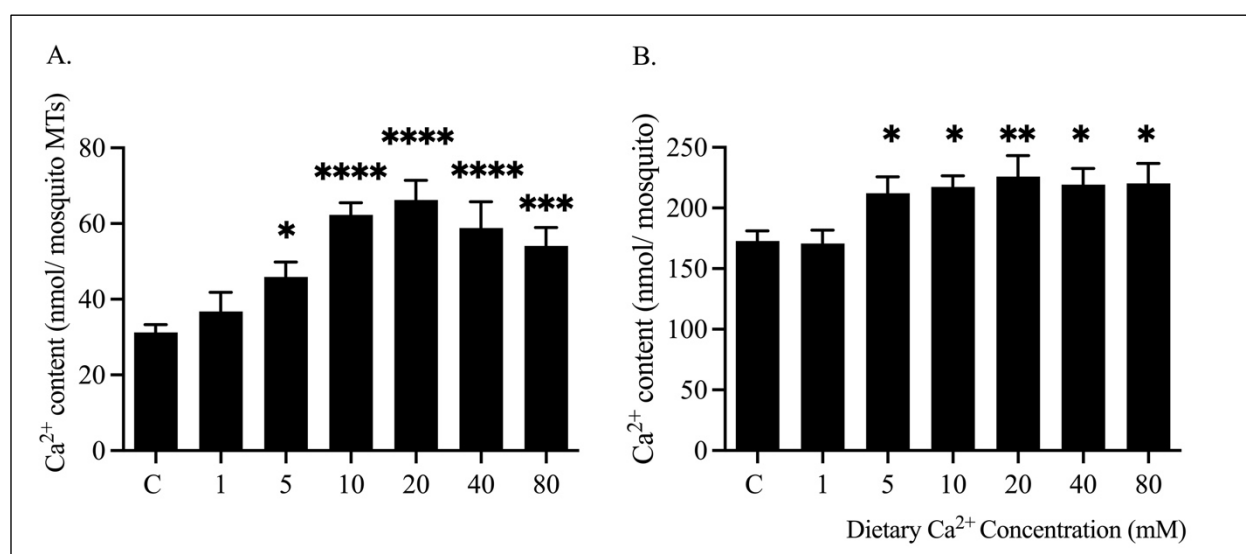
632
633   Figure 1. Effects of dietary Ca^{2+} treatments on the content of Ca^{2+} in Malpighian tubules (MTs)

634   (A) and whole bodies (B) of adult females. Asterisks indicate significant differences between

635   control (C) and each treatment group as determined by ordinary one-way ANOVA and Holm-

636   Sidak post hoc tests ($p < 0.05$). Values are mean $\pm$ s.e.m. For Malpighian tubules, n = 16, 5, 7, 7,

637   8, 8, and 7, respectively, for C, 1, 5, 10, 20, 40, and 80 mM Ca^{2+} treatments; for whole bodies, n =

638   15, 5, 7, 7, 8, 7, and 6, respectively, for C, 1, 5, 10, 20, 40, and 80 mM Ca^{2+} treatments.
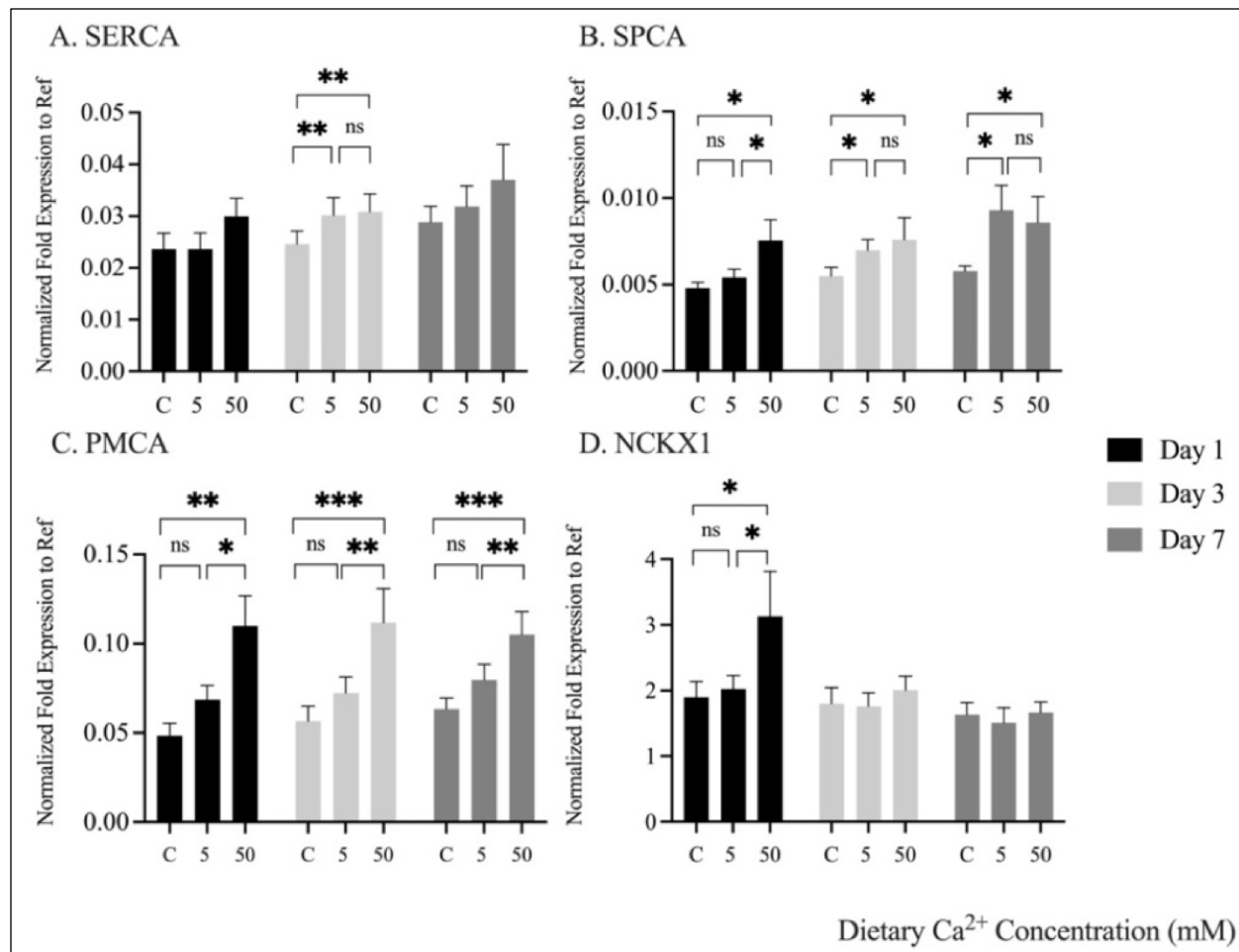
Figure 2. Effects of dietary Ca^{2+} treatments on *SERCA* (A)*, SPCA* (B)*, PMCA* (C), and *NCKX1* (D) mRNA levels in *Ae. aegypti* Malpighian tubules at days 1, 3, and 7 (indicated by black, light grey, and dark grey bars separately). Asterisks indicate differences among means within a time point as determined by a randomized block one-way ANOVA and Fisher's LSD tests ($p < 0.05$). C = control. Values are mean ± s.e.m; n = 5 replicates.
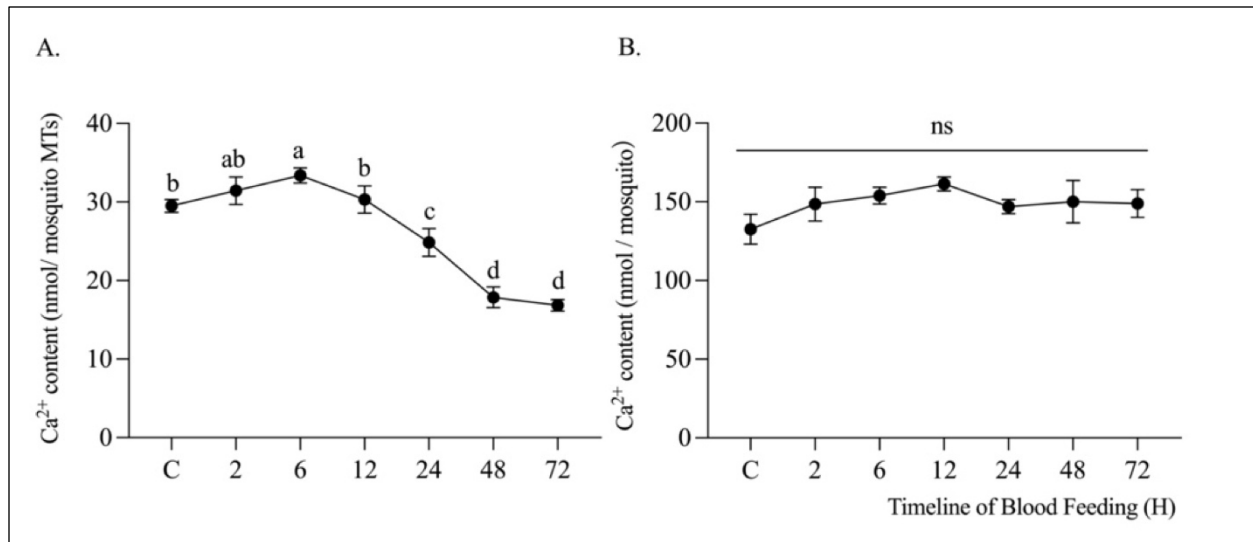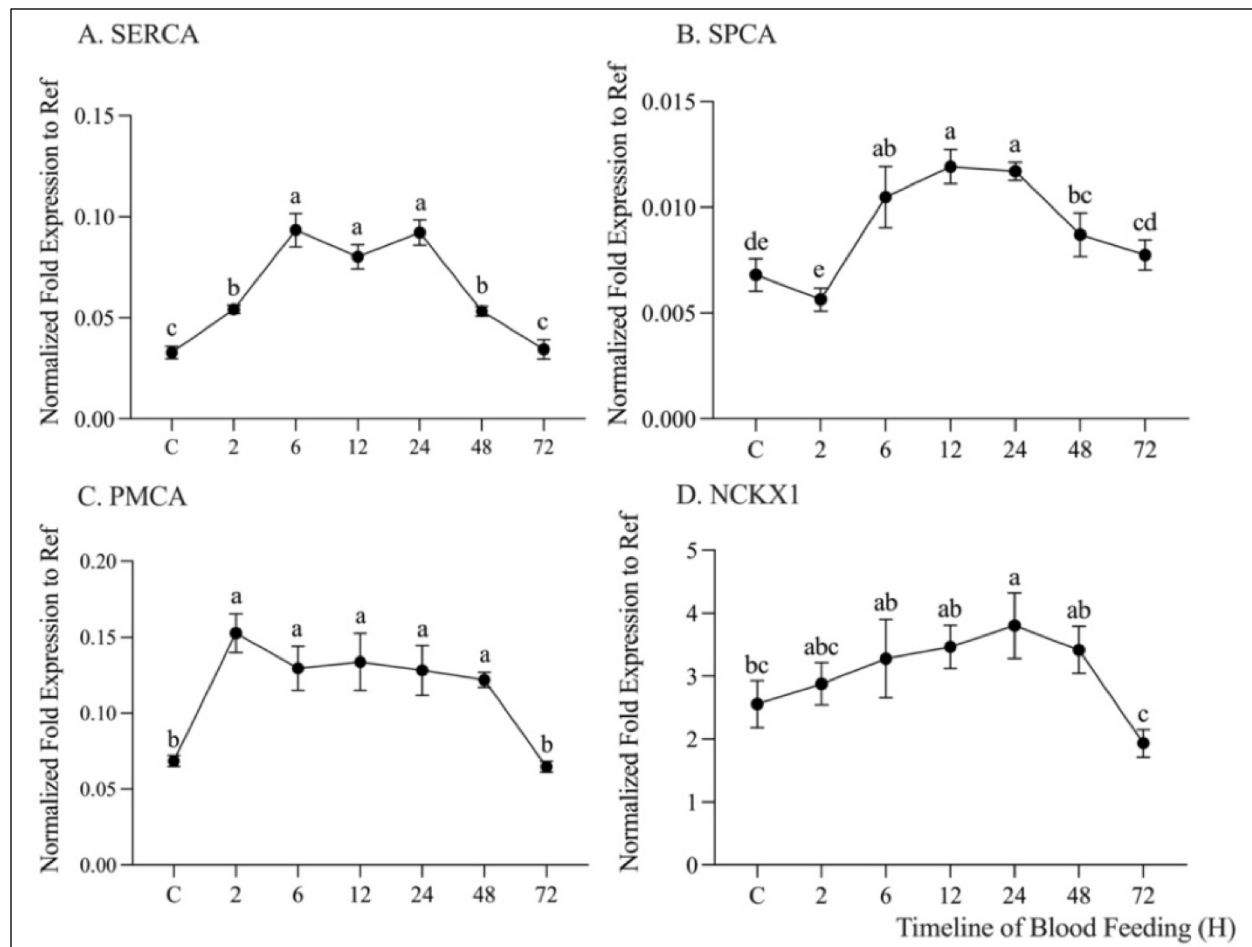
Figure 3. Effects of blood feeding on the content of Ca^{2+} in Malpighian tubules, MTs (A) and whole bodies (B). Lower-case letters indicate statistical categorizations of the means as determined by a randomized block one-way ANOVA and Fisher's LSD tests ($p < 0.05$). Values are mean ± s.e.m; n = 5 replicates.

650

Figure 4. Effects of a blood meal on *SERCA* (A)*, SPCA* (B)*, PMCA* (C), and *NCKX1* (D) mRNA abundance in *Ae. aegypti* Malpighian tubules before (C) and at several time points post blood feeding. The relative mRNA expressions of *SERCA*, *SPCA*, and *PMCA* were log-transformed to fit the assumption of normality before statistical analysis (for clarity, data shown are not log transformed). Lower-case letters indicate statistical categorizations of the means as determined by a randomized block one-way ANOVA and Fisher's LSD tests ($p < 0.05$). Values are mean $\pm$ s.e.m; n = 5 replicates.

658
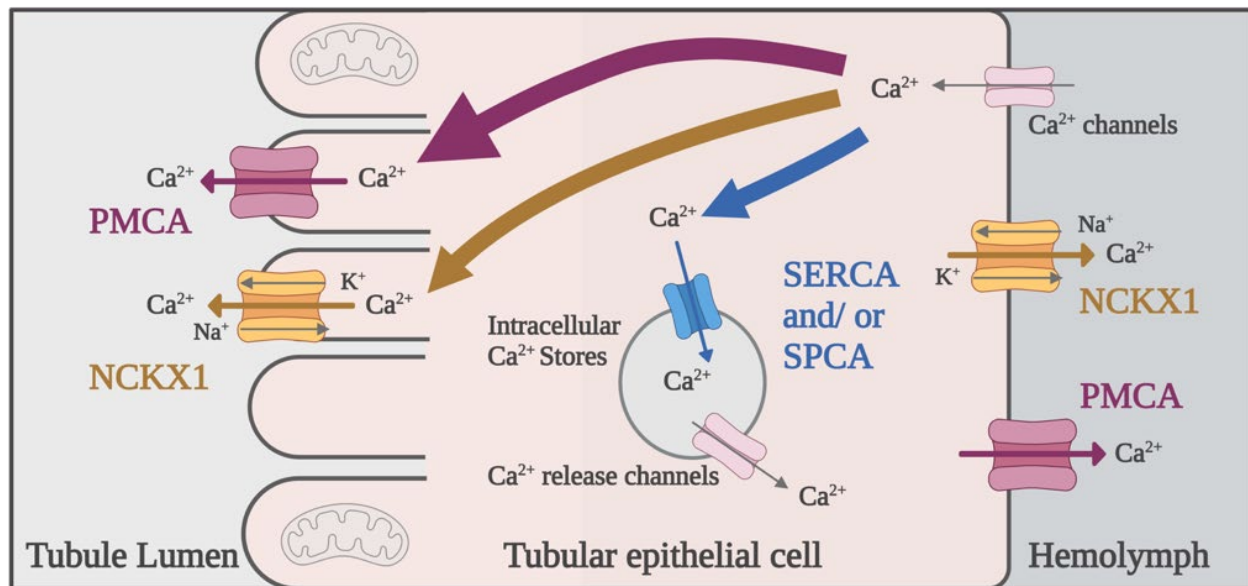
Figure 5. Hypothesized model of Ca^{2+} transporting mechanisms in mosquito Malpighian tubule epithelial cells when fed 10% sucrose with elevated Ca^{2+}. Putative localization of transporters is adopted from the Browne and O'Donnell (2018a) model of Ca^{2+} transport in *A. domesticus*. Magenta, yellow, and blue arrows represent the possible Ca^{2+} transport pathways mediated by apical/basolateral PMCA, apical/basolateral NCKX1, and intracellular SERCA/SPCA, respectively. Grey arrows represent putative mechanisms of Ca^{2+} influx (Ca^{2+} channels) and intracellular release (Ca^{2+} release channels) not examined in the present study. Thickened arrows represent our interpretations of the up-regulated mRNAs in Figure 2.
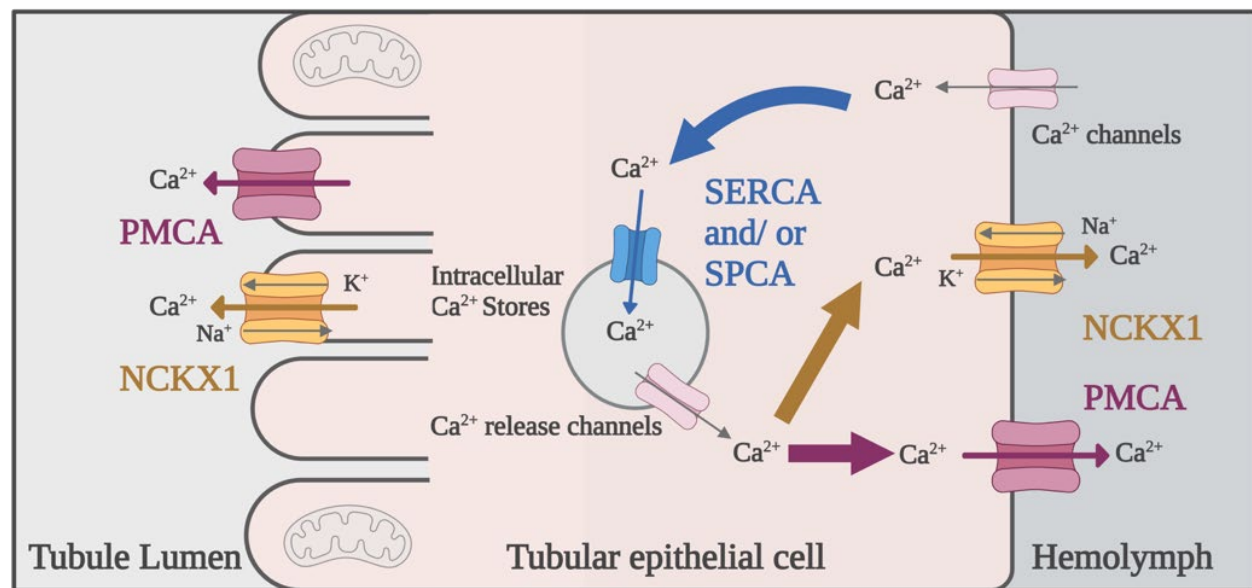
Figure 6. Hypothesized model of Ca^{2+} transporting mechanisms in mosquito Malpighian tubule epithelial cells during Phase 1 and 2 (i.e., 0-48 h) PBF. Putative localization of transporters is adopted from the Browne and O'Donnell (2018a) model of Ca^{2+} transport in *A. domesticus*. Magenta, yellow, and blue arrows represent the possible Ca^{2+} transport pathways mediated by apical/basolateral PMCA, apical/basolateral NCKX1, and intracellular SERCA/SPCA, respectively. Grey arrows represent putative mechanisms of Ca^{2+} influx (Ca^{2+} channels) and intracellular release (Ca^{2+} release channels) not examined in the present study. Thickened arrows represent our interpretations of the up-regulated mRNAs in Figure 4.

8. Appendices

Table S1. Forward and reverse primers used in qPCR.

Gene	Vectorbase Accession #	Forward Primer (5′-3′)	Reverse Primer (5′-3′)
SERCA	AAEL006582	TGCTGTGGGTCAACTTGGTT	CATCAGCCTTACGTGGTGGT
SPCA	AAEL003518	GTACCCCTTCAGTTCCGAGC	GGCACCCTTGACGAAGAAGA
PMCA	AAEL019458	TCCAGTCACGAATCGAAGGC	AGATGTCGCCCACCACAATT
NCKX1	AAEL004805	GTGGTAGGATCGGCTGTGTT	GGGCCACCATCGTAGTTG
Actin	AAEL011197	CGTTCGTGACATCAAGGAAA	GAACGATGGCTGGAA GAG AG
RPS17	AAEL004175	AAGAAGTGGCCATCATTCCA	GGTCTCCGGGTCGAC TTC

679 **Table S2.** Effects of dietary Ca^{2+} in 10% sucrose on the Ca^{2+} content increases in mosquito whole

680 bodies and Malpighian tubules (data are calculated from Figure 1; values are mean ± s.e.m), and

681 the percentage of the whole body Ca^{2+} increase attributed to Malpighian tubules. Data are only

682 shown for Ca^{2+} treatments that resulted in significant increases to whole bodies and Malpighian

683 tubules (see Figure 1).

CaCl$_2$ Concentration (mM) in 10% sucrose	Whole body Ca^{2+} increase (nmol)	Malpighian tubule Ca^{2+} increase (nmol)	Percentage of whole body Ca^{2+} increase attributed to Malpighian tubules (%)
5	39.5 ± 13.5	14.7 ± 3.9	37.1 ± 10.0
10	44.6 ± 9.3	31.0 ± 3.2	69.6 ± 7.2
20	53.3 ± 17.3	35.0 ± 5.2	65.7 ± 9.8
40	46.5 ± 13.5	27.6 ± 6.9	59.4 ± 14.9
80	47.6 ± 16.6	22.9 ± 4.85	48.1 ± 10.2

684

Table S3. Estimated total amount of Ca^{2+} ingested per mosquito after 6 days of feeding on elevated dietary Ca^{2+} in 10% sucrose compared to the increase of Ca^{2+} in mosquito whole bodies (Supplemental Table 2). Amount of Ca^{2+} ingested was calculated by the product of Ca^{2+} concentration and volume ingested. The difference between the estimated ingestion and whole body increase is hypothesized to be excreted. Values are means ± s.e.m.

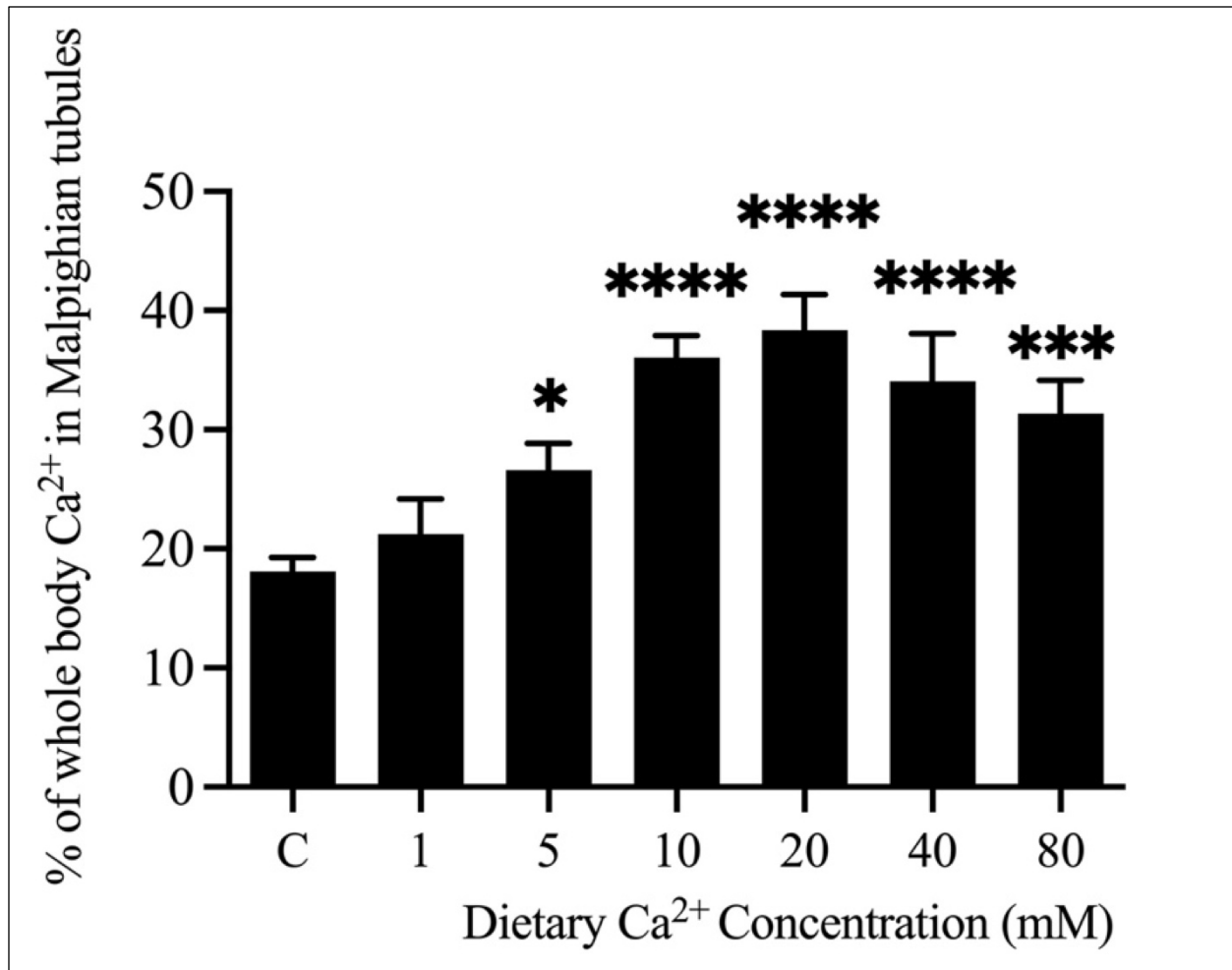| $CaCl_2$ Concentration (mM) in 10% sucrose	Volume of 10% sucrose ingested over 6 days (µL/mosquito)	Amount of Ca^{2+} ingested over 6 days (nmol/mosquito)	Whole body Ca^{2+} increase (nmol/mosquito)	Hypothesized Ca^{2+} Excreted (nmol/mosquito)
5	11.4 ± 1.2 (n = 5)	56.8 ± 6.2	39.5 ± 13.5	≈ 17.3
10	13.1 ± 0.6 (n = 5)	130.9 ± 5.8	44.6 ± 9.3	≈ 86.3
20	7.8 ± 0.4 (n = 5)	155.5 ± 7.2	53.3 ± 17.3	≈ 102.2
40	6.1 ± 0.8 (n = 5)	245.0 ± 31.1	46.5 ± 13.5	≈ 198.5
80	7.5 ± 2.3 (n = 5)	436.5 ± 98.5	47.6 ± 16.6	≈ 388.9

Figure S1. Percentage of whole body Ca^{2+} levels detected in Malpighian tubules. C = control group and numbers indicate Ca^{2+} concentration (mM) in treated groups. Percentages were determined by dividing the tubule Ca^{2+} content for each biological replicate by the respective mean whole body Ca^{2+} content within a group. Values are mean ± s.e.m; n = 16, 5, 7, 7, 8, 7, and 6 respectively, for C, 1, 5, 10, 20, 40, and 80 mM Ca^{2+} treatments
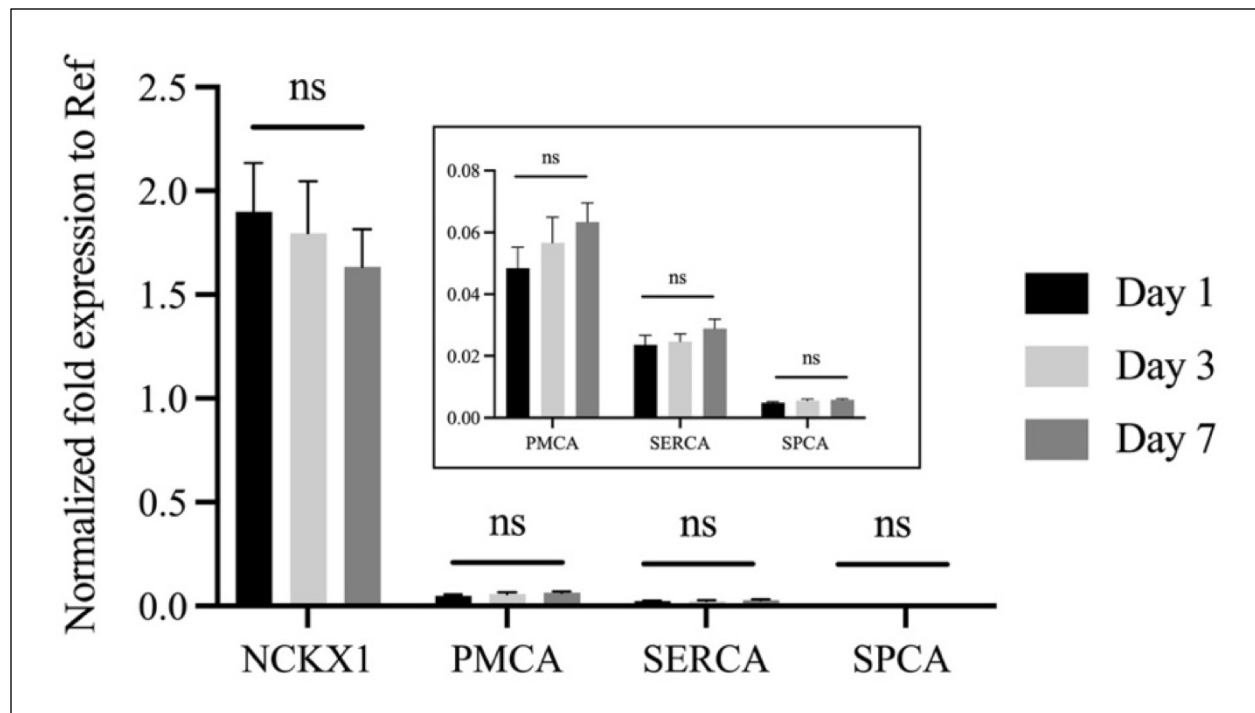
Figure S2. Relative mRNA expression of Ca^{2+}-transporters in Malpighian tubules of controls; inset shows magnified view for *PMCA*, *SERCA*, and *SPCA*. Black, light grey, and dark grey bars respectively represent the relative expression values of control groups at 1 d, 3 d, and 7 d after feeding on 10% sucrose diets. PMCA: p = 0.1553 (Kruskal Test); SERCA, SPCA, and NCKX: p = 0.4294, 0.2492, 0.7074 (Ordinary One-way ANOVA). Values are mean ± s.e.m; n = 5 replicates.